

Ergodicity in hard-ball systems and Boltzmann's entropy

Zhigang Zheng,¹ Gang Hu,^{2,1} and Juyuan Zhang³

¹Physics Department, Beijing Normal University, Beijing 100875, China

²Center of Theoretical Physics, China Center for Advanced Science and Technology (World laboratory), Beijing 8730, China

³Physics Department, Siping Teacher's College, Jilin, China

(Received 6 September 1995)

The ergodic property of the hard-ball systems is investigated numerically by comparing the microcanonical single-particle distributions and the corresponding numerical results in two- and three-dimensional cases. A Boltzmann-entropy-like quantity $H(n_c)$ is defined and its evolution is discussed. The deviation of this entropy from the equilibrium value obeys a power decay law in the long time limit, and the origin of this tail is explored heuristically. [S1063-651X(96)07704-5]

PACS number(s): 05.45.+b, 02.50.-r

I. INTRODUCTION

Both the verification of the Boltzmann-Sinai ergodic hypothesis and the understanding of the mixing behavior of the physical systems are substantial questions of the foundations of statistical physics [1,2]. Ergodicity means roughly the exploration of the energy surface $H(p; q) = E$ by a typical trajectory. Krylov suggested that the exponential instability property should be responsible for the cause of ergodicity in a model dynamical system [3]. Mathematically, the ergodic property is characterized by the positive Kolmogorov-Sinai entropy, which is related to all positive Lyapunov exponents [4,5]. It has been shown that for the ergodic Hamiltonian systems, ergodicity (chaos) provides the validity of the laws of equilibrium thermodynamics and statistical mechanics [6,7]. In general, nonintegrable systems involve two classes [8]. One class contains the completely chaotic systems, such as billiard systems [9], which generally have hard convex surfaces or hard surfaces with irregular shape (dispersing or semidispersing property). Hard surfaces lead to nonsmooth Hamiltonians. In these systems, infinite number of periodic but unstable orbits can be found. One of the most interesting models in mathematics is the Sinai billiard [4,5], i.e., a point particle moves freely in a given domain and collides elastically with the hard walls, thus the topology of the boundary is the most important factor. Slight asymmetry may lead to ergodicity, mixing and even a K system. The other class comprises of those with smooth Hamiltonians, these systems contain quasiperiodic [Kolmogorov-Arnold-Moser (KAM)], chaotic and stable (unstable) orbits. The study of this class of systems is the main subject of chaos in the conservative Hamiltonian systems. In traditional hypotheses, ergodic properties are always connected to a large number of degrees of freedom and are difficult to prove.

On the other hand, a very old but physically important model is the hard-ball gas in a box, which may correspond to a complicated billiard [1]. Consider the motion of N balls of radius r in a box (a cube, or, more generally, in a specific domain) $Q \in R^d$ ($d \geq 2$), the balls interact elastically among themselves and with the (piece-wise smooth) boundary ∂Q , then the Hamiltonian reads

$$H = \sum_i p_i^2 / 2m_i, \quad (1)$$

where $p_i^2 = p_{ix}^2 + p_{iy}^2$ for the two-dimensional (2D) motion and $p_i^2 = p_{ix}^2 + p_{iy}^2 + p_{iz}^2$ for the three-dimensional (3D) case.

The famous Boltzmann-Sinai ergodic hypothesis claims that the Hamiltonian systems of an arbitrary number ($N \geq 2$) of the elastic hard balls on the ν ($\nu \geq 2$) dimensional torus are ergodic on connected components of submanifolds of the phase space where the trivial integral of motion is constant energy. In fact, this hypothesis stimulated the initial development of the notions of the ergodic theory itself in the works of Boltzmann [10] and Gibbs [11]. The outstanding contribution in the approach to this problem was made by Ya. G. Sinai in his papers [4,5], where some powerful methods were developed, and he proved the ergodicity of the two-ball system on ν ($\nu \geq 2$) torus. Recently, the method proposed by Kramli, Simanyi, and Szasz [12-16] is also very important in proving the ergodicity for the hyperbolic dynamical systems with singularities, and they have proved the ergodicity for the three-disk systems on a two-torus, four-disk systems on ν ($\nu \geq 3$)-torus and N -disk system on ν ($\nu \geq N$)-torus. However, the proof of the ergodicity for a system of an arbitrary number of elastically interacting balls is still an open problem. Theoretical difficulty emphasizes the importance of the numerical investigations.

Ergodicity in one-dimensional hard-ball systems has been numerically investigated by Ackland [17], where periodic boundary condition was used. Investigation of two- and three-dimensional hard-ball systems is also very important because they are more physically significant. In this paper, we shall test the ergodicity of the two- and three-dimensional hard-ball systems by comparing the microcanonical distribution (single-particle reduced distribution) and numerically statistical results. Similar method has been used in our previous work [18]. As is expected, we find the good ergodic property of this system for the different number of balls ($N \geq 2$) in the two- and three-dimensional cases.

On the other hand, as we mentioned from the beginning, a deeper understanding of the mixing behavior is necessary from the point of view of physics [9], such as the rate of mixing, the evolution of physical quantities, and the equipartition of energy to each degree of freedom. These are rarely discussed quantitatively in mathematics, but important in physics. In order to explore the mixing behavior of the hard-ball systems, we introduce a Boltzmann-entropy-like quan-

tity $H(n_c)$, which will be defined in the Sec. III, and investigate its evolution. Because we are interested in the statistical behavior of our systems, long time evolution is required. Therefore short-time effects will not be considered here. We find that this Boltzmann's entropy evolves to its equilibrium value monotonically. For a given mixing Hamiltonian system, the rate of a single trajectory covering the entire energy surface is usually very slow in the long time limit. Numerical investigation reveals that a long time tail of the power-law decay of the Boltzmann's entropy exists. We shall also study the origin of this tail numerically, and show that the neutral boundary (i.e., regular motion segments) should be responsible for this long tail.

II. ERGODICITY OF HARD-BALL SYSTEMS

For simplicity, we assume that all balls are identical, i.e., have the same inertial mass m and the same radius r . The hard-ball potential and the hard reflecting walls enable us to describe the dynamics just by a series of discrete collisions, and this greatly simplifies our numerical simulation. At each step, we only need to compute the time of the next collision between each pair of balls and between the balls and the walls, and then choose the shortest time as the time step to move all the balls.

If the ball-wall collision occurs, we just use the elastic reflection rule: $p_{i\alpha} \rightarrow -p_{i\alpha}$, where i denotes the i th ball and α represents the direction perpendicular to the wall, i.e., x , y , or z . If the ball-ball collision occurs, for example, between the i th and the j th one, by using the conservation law of kinetic energy and momentum, we have the velocities after the collision:

$$\begin{aligned}\vec{v}_i^c &= \vec{v}_i + \frac{2m_j}{m_i + m_j} (\vec{v}_j - \vec{v}_i) \cdot \frac{\vec{r}}{|\vec{r}|^2} \vec{r}, \\ \vec{v}_j^c &= \vec{v}_j - \frac{2m_i}{m_i + m_j} (\vec{v}_j - \vec{v}_i) \cdot \frac{\vec{r}}{|\vec{r}|^2} \vec{r},\end{aligned}\quad (2)$$

where $\vec{r} = \vec{r}_j - \vec{r}_i$, and \vec{r}_i, \vec{r}_j denote the positions of the mass centers of the i th and j th balls, respectively, \vec{v}_i and \vec{v}_i^c the velocities of the i th ball before and after the collision.

It should be noted that in this system the conservation of momentum is violated, for the balls collide with the wall. This will strengthen the degree of ergodicity (chaos), but the conservation of the magnitude of the momentum (i.e., $|\vec{p}_i|$) at the ball-wall collisions will reduce the mixing rate, i.e., slow down the evolution to the equilibrium state. In the following subsections, we will discuss the ergodic property of the hard-ball systems in both momentum space and configuration space.

A. Ergodicity in the momentum space

The single-particle momentum probability distribution may be explicitly derived from the microcanonical ensemble. Taking the two-dimensional motion, for an example, if the hard-ball system is ergodic, the microcanonical ensemble distribution should be

$$\Delta W \propto \Delta p_{1x} \Delta p_{1y} \Delta x_1 \Delta y_1 \dots \Delta p_{Nx} \Delta p_{Ny} \Delta x_N \Delta y_N = \Delta \Gamma, \quad (3)$$

where ΔW is the probability of a trajectory entering a phase volume unit $\Delta \Gamma$ between the $E \rightarrow E + \Delta E$ energy shell. On the energy surface $\Delta E \rightarrow 0$. By eliminating $x_1, y_1 \dots x_N, y_N$ and p_{Nx}, p_{Ny} ($N \geq 2$), we obtain the single-particle momentum distribution (the inertial mass is normalized to 1)

$$\rho_2(p) = C_2 p (2E - p^2)^{N-2}, \quad (4a)$$

where C_2 is a normalization constant, which reads

$$C_2 = 2(N-1)/(2E)^{N-1}, \quad (4b)$$

and p is the absolute value of \vec{p}_i . Here the subscripts of the momentum are omitted because all balls have the same distribution. For the three-dimensional case, the reduced single-particle momentum distribution is expressed by

$$\rho_3(p) = C_3 p^2 (2E - p^2)^{3(N-1)/2-1}, \quad (5a)$$

and the normalization constant reads

$$C_3 = (3N-1)/[(2E)^{(3N-2)/2} I_{3N-4}], \quad (5b)$$

where

$$I_i = \frac{i-1}{i} I_{i-2} = \begin{cases} \frac{i-1}{i} \frac{i-3}{i-2} \dots \frac{4}{5} \frac{2}{3} & (\text{odd } i) \\ \frac{i-1}{i} \frac{i-3}{i-2} \dots \frac{3}{4} \frac{1}{2} \frac{\pi}{2} & (\text{even } i), \end{cases} \quad (5c)$$

and $I_1 = 1, I_0 = \pi/2$.

After scaling, the average energy per ball e (i.e., the temperature of the system) is an irrelevant control parameter for the system behavior. Therefore we fix $e = 50\,000$ throughout the paper without losing any generality ($E = Ne$).

From Fig. 1(a) to 1(c), we compare the numerical and theoretical reduced single-particle momentum distributions $\rho(p)$ for the different numbers of balls ($N=2, 6, 12$) in the two-dimensional case. Here every numerical $\rho(p)$ is obtained by running a single trajectory from an arbitrary initial condition, and 5×10^5 data are collected. We find that the numerical curves (solid sawlike) are in quite good agreement with theoretical ones (smooth dashed); this indicates the systems reach good ergodicity after a long time. From Fig. 2(a) to 2(c), the numerical and theoretical distributions for $N=2, 6, 12$ in the three-dimensional case are given, and quite good ergodicity is obtained again for all these systems. In fact, they are even mixing, K system as pointed out by Sinai and others [1,4,5,12-16]. The dispersing property of the balls gives the exponential instability, i.e., any two closed trajectories will depart exponentially. However, because of the existence of the neutral boundary (not dispersing), the evolution of the system will not be an exponential one in the long time regime, as we shall see in the following sections.

B. Ergodicity in the configuration space

The behavior of the distribution in the configuration space is also interesting. Let us consider a two-ball system in a two-dimensional space. We can derive the reduced one-particle configuration distribution $P(x,y)$ in the x - y plane from the microcanonical ensemble (3). In order to get the analytical form of $P(x,y)$, we may fix one ball (say, ball 1)

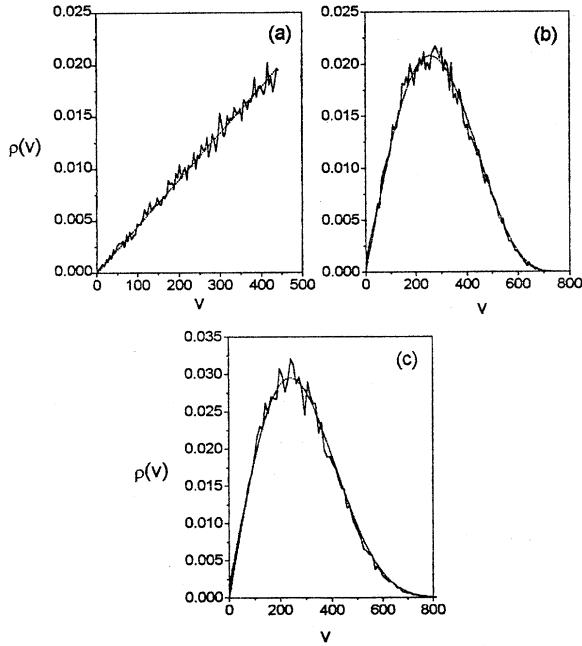


FIG. 1. Numerical (solid-saw-like) and theoretical (short-dotted) single-particle momentum distributions for the two-dimensional motion of the hard-ball systems with a different number of balls: (a) $N=2$, (b) $N=6$, (c) $N=12$. Good agreement shows ergodicity of 2D hard-ball systems. $L=100$, $E=50\,000 \times N$ (the same L and E are taken in all the following figures), $r=5$, and 5×10^5 collisions are used for producing each simulation curve.

and compute the accessible area of the other ball (ball 2) by a geometric consideration. From (3) we may find that $P(x_1, y_1) \propto \iint dx_2 dy_2$, where (x_2, y_2) denotes the center of mass of ball 2. Simple geometric consideration shows that there exists a critical radius $r_c = L/6$, where L is the length of the box. When $r \leq r_c$, a direct computation gives rise to

$$P(x, y) = A^{-1} [(L - 2r)^2 - 4\pi r^2] \quad \text{for } |x| \leq L/2 - 3r$$

$$\text{and } |y| \leq L/2 - 3r;$$

$$P(x, y) = A^{-1} [(L - 2r)^2 - 4r^2(\pi - \theta) - 2r^2 \sin 2\theta]$$

$$\text{for } |x| > L/2 - 3r \text{ or } |y| > L/2 - 3r;$$

$$P(x, y) = A^{-1} [(L - 2r)^2 - 2r^2(3\pi/2 - \alpha - \beta) - r^2(\sin 2\alpha$$

$$+ \sin 2\beta + 4 \cos \alpha \cos \beta)]$$

$$\text{for } |x| > L/2 - 3r \text{ and } |y| > L/2 - 3r, \quad (6)$$

where $\cos \theta = (L/2 - r - |x|)/2r$ in the region $|x| > L/2 - 3r$ and $|y| < L/2 - 3r$; and $\cos \theta = (L/2 - r - |y|)/2r$ in the region $|x| < L/2 - 3r$ and $|y| > L/2 - 3r$. Moreover, we have $\cos \alpha = (L/2 - r - |x|)/2r$, $\cos \beta = (L/2 - r - |y|)/2r$. A is a normalization constant.

For the case $r > r_c$, one should consider more geometric cases and an analytical expression of $P(x, y)$ is still available

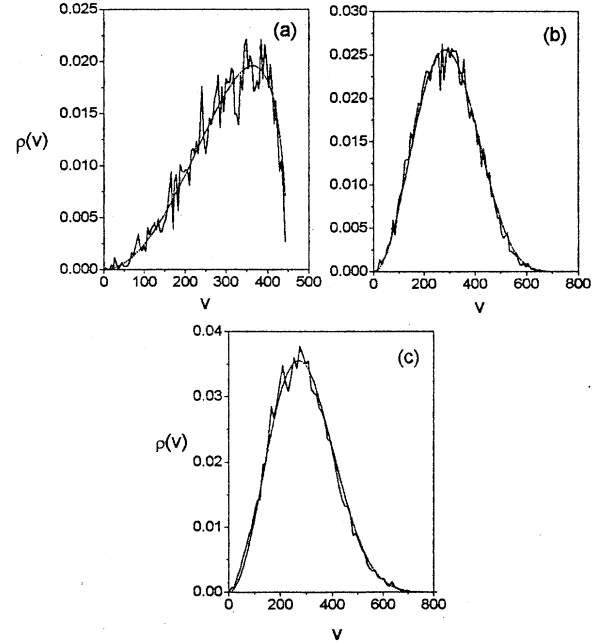


FIG. 2. The same as Fig. 1 with the space dimension changed from two to three. (a) $N=2$, (b) $N=6$, (c) $N=12$. Again good agreement shows ergodicity of 3D hard-ball systems. Numerical $\rho(v)$ is computed, based on the data at all ball-ball and ball-wall collisions.

while tedious. Hence we do not give this long expression here, but some theoretical results are still presented in Fig. 3(d) by the dotted curve.

For a single x -variable distribution, we have $P(x) = \int P(x, y) dy$. The comparison between the numerical counting distribution and the theoretical reduced equilibrium distribution is shown in Fig. 3(a)–3(d). It is obvious that for long enough time, the ergodicity can be reached. For small r , a long horizontal segment exists. In the small r limit, i.e., $r \rightarrow 0$, the influence of the limitation $|\vec{r}_i - \vec{r}_j| \geq 2r$ is negligible, and $P(x) \rightarrow \text{const}$. As r increases, the width of the horizontal segment decreases. At $r = r_c$, the horizontal part disappears. For large r , the two balls would spend a major portion of time in the corner region, then $P(x)$ has a large probability near the boundaries, and a small probability in the central region. Numerical simulations support our expectation. In Figs. 3(a), 3(b), horizontal segments are presented, and in Fig. 3(d), $r = 20 > r_c$, the horizontal part disappears.

The same algorithm can be carried out for the many-particle systems. However, as N increases, the computation becomes more and more tedious, while the general conclusion is the same. We will not go further for $N > 2$.

III. BOLTZMANN'S ENTROPY AND LONG TIME TAIL

As we mentioned above, the hard-ball system is ergodic and mixing, so it will evolve to the equilibrium state from a typical initial state. In statistical mechanics, one often uses Boltzmann's entropy to describe the relaxation of a dynamical system to the equilibrium state. To characterize the mixing behavior (relaxation process), we introduce a Boltzmann-

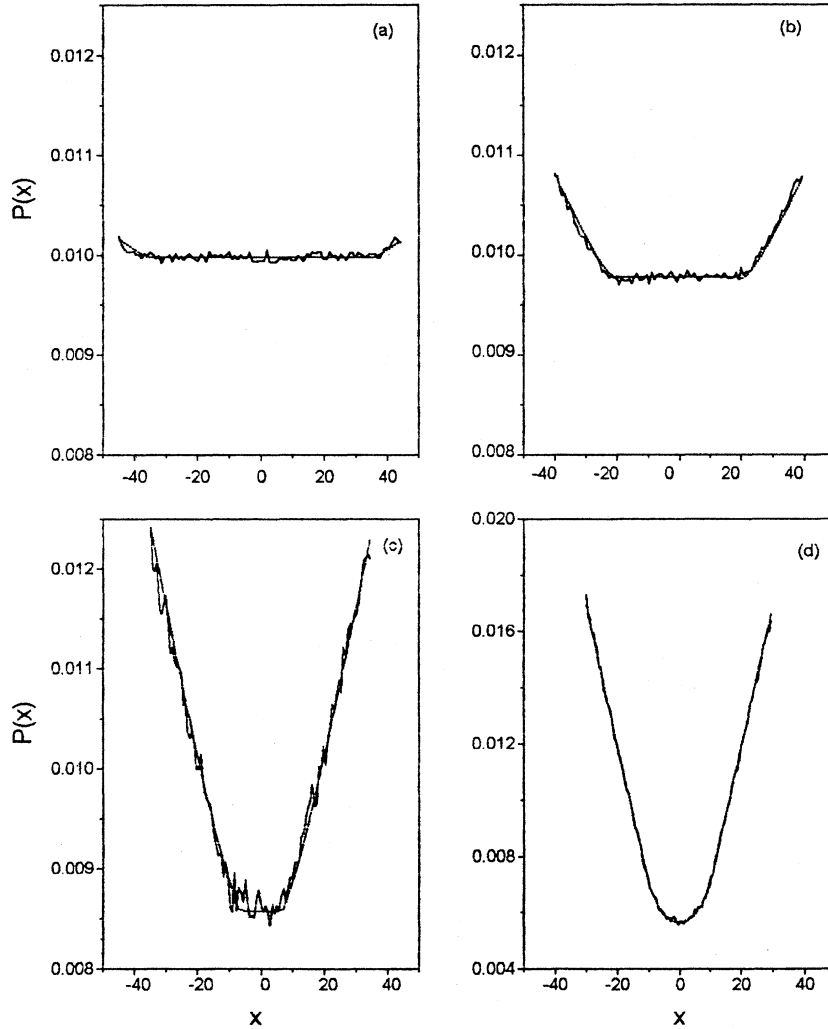


FIG. 3. Numerical (solid-saw-like) and theoretical (short-dotted) single-particle configuration distributions for the two-dimensional motion of two hard-ball systems with different radius: (a) $r=5$, (b) $r=10$, (c) $r=15$, (d) $r=20$. Good agreement shows ergodicity of 2D two hard-ball systems.

entropy-like quantity $H_p(n_c)$, which is defined as

$$H_p(n_c) = \int \rho_{n_c}(p) \ln \rho_{n_c}(p) dp. \quad (7)$$

Here n_c denotes the number of collisions (including both ball-ball and ball-wall collisions), and $\rho_{n_c}(p)$ represents the reduced distribution after the n_c th collision, computed based on all collisions. We call this quantity a Boltzmann-entropy-like one because it has the form similar to the standard Boltzmann's entropy in the many-body systems, but it is still slightly different from the standard definition of a Boltzmann's entropy because the latter considers the distribution in the entire single-particle phase space including both configuration and momentum variables. However, for convenience, we simply call Eq. (7) the Boltzmann's entropy in the following discussions. Another reason for introducing this quantity is that it can be easily computed numerically, and it also describes the mixing behavior, as we may see in the following discussions.

Note that here the Boltzmann's hypothesis of the molecular chaos is violated, i.e.,

$$\rho_{n_c}(p_1, p_2) \neq \rho_{n_c}(p_1) \rho_{n_c}(p_2). \quad (8)$$

When $n_c \rightarrow \infty$, $H_p(n_c) \rightarrow H_{p0}$, where H_{p0} is the Boltzmann entropy at the equilibrium state. In Fig. 4, the evolution of $H_p(n_c)$ is plotted. It is shown that the Boltzmann's entropy is a monotonically decreasing function, this monotonicity exists even without the Boltzmann's chaotic assumption and with the finite ball volume. We also find that the system reaches nearly equilibrium within a short time and quite a long time is spent in reaching the perfect equilibrium state. This shows that the rate for a trajectory covering the energy surface is very slow in the long time limit.

The radius of the hard-balls r (or, the volume of the box L^d) may affect the relaxation process of the system. The larger the radius is, the faster the system reaches the equilibrium state. Taking the two-dimensional two-ball system, for example, the length of the box is $L=100$. We count the first 10 000 collisions. Then the ratio of the number of the ball-wall collisions N_{bw} to the number of the ball-ball collisions N_{bb} is 9070/930 for $r=5$, while 8318/1682 for $r=10$, and 6966/3034 for $r=20$, indicating the number of the ball-ball collisions increases with increasing r for a given number of

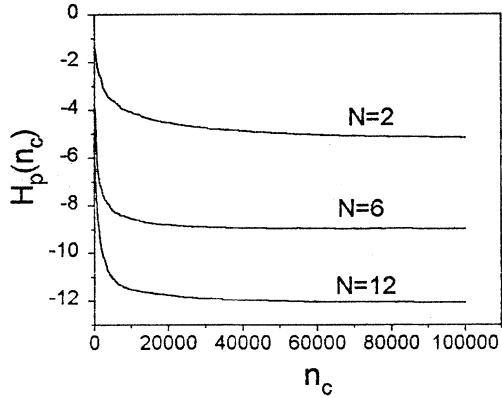


FIG. 4. The evolution of the Boltzmann's entropy $H_p(n_c)$ in the 2D case for the number of balls the same as in Fig. 1. The entropy decreases monotonically with increasing time.

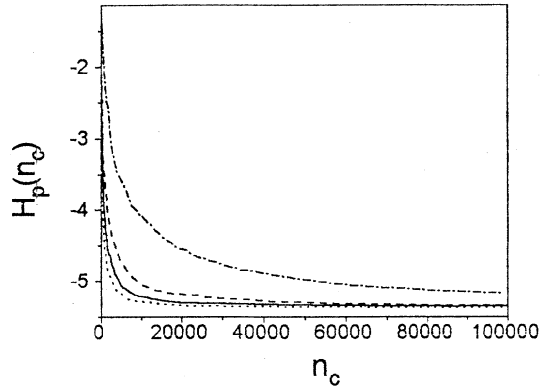


FIG. 5. The evolution of Boltzmann's entropy $H_p(n_c)$ for the 2D and two-ball case for the different radius of balls. From upper to lower we take $r=1, 5, 10, 20$, respectively. The mixing rate increases with increasing r .

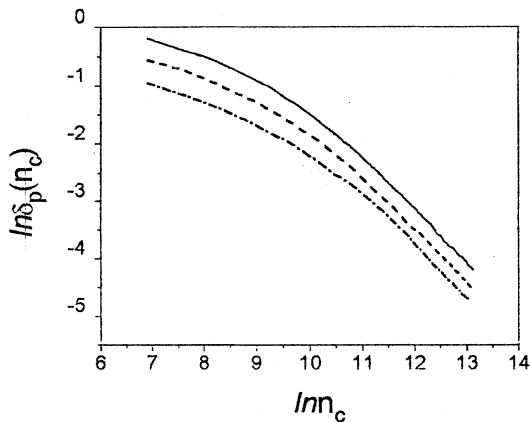


FIG. 6. The log-log (with the base $e=2.718\ 281\ 83\dots$) histogram of $\delta_p(n_c)$ vs n_c in the two-dimensional motion case for the different number of balls: $N=2$ (dot-dashed), 6 (dashed), 12 (solid). Long straight segments exist in the long time limit, indicating the power-law decay of $\delta_p(n_c)$.

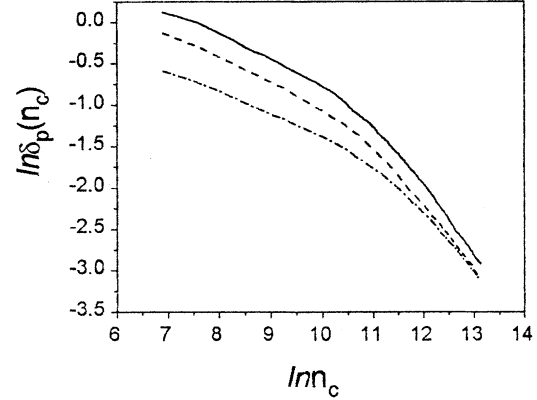


FIG. 7. The same as Fig. 6 in the three-dimensional motion case. Long straight segments and then the power-law decay of $\delta_p(n_c)$ also exist in the long time limit.

total collisions. In Fig. 5, the evolution of $H_p(n_c)$ is shown for the 2D two-ball system for a different r , we find that the mixing rate in momentum space increases with increasing r . However long tails still exist for a different r .

While the rate of covering the constant energy surface is very slow, what law is obeyed in this long time limit? We use the difference $\delta_p(n_c) = |H_p(n_c) - H_{p0}|$ to study this limit. In Figs. 6 and 7, we plot the log-log (with the base $e=2.718\ 281\ 83\dots$) histograms of $\delta_p(n_c)$ for the 2D and 3D cases and find that the long straight segments exist, which shows a power-law decay of $\delta_p(n_c)$ [or, $H_p(n_c)$] for large n_c (long time).

The long tail behavior has been explored by using various methods, and in different systems [20–27]. Systems with very strong statistical properties (K systems) are characterized by exponential instability of motion, which indicates the

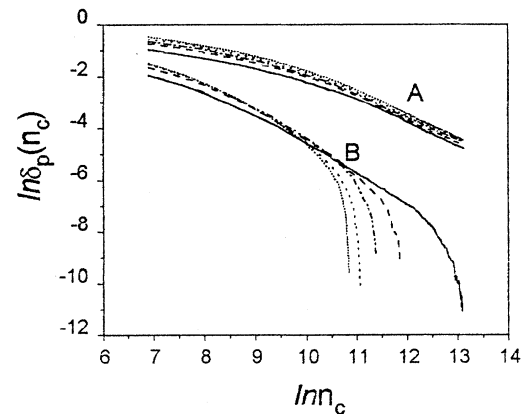


FIG. 8. The log-log histogram of $\delta_p(n_c)[\delta_p(n'_c)]$ vs $n_c(n'_c)$ in the two-dimensional motion case for the different number of balls: $N=2$ (solid), 4 (dashed), 5 (dot-dashed), 6 (dotted), 7 (short-dotted), where group A is the same as in Fig. 5, and group B (n'_c) represents the number of collisions between a given ball with the other balls only. The curves B drop dramatically, which shows what happens when the influence of the ball-wall collisions (i.e., long regular motion) is lifted.

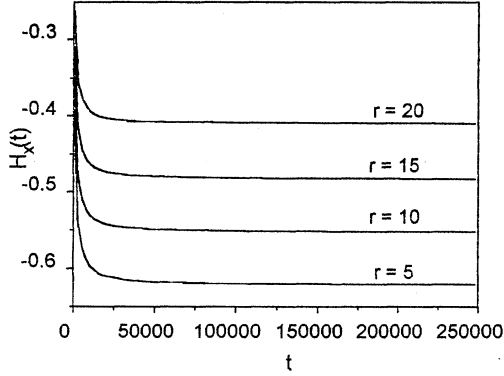


FIG. 9. The evolution of the Boltzmann's entropy $H_x(t)$ for the 2D and two-ball case for the different radius of the balls. From upper to lower we take $r=5, 10, 15, 20$, respectively. It is shown that $H_x(t)$ decreases monotonically and approaches its equilibrium value as time goes to infinity.

exponential loss of the memory of the initial state. However, for a K system approaching an equilibrium state, the picture of a transport phenomena (i.e., an exponential decay of correlation functions) given by Boltzmann is not completely correct [19]. Boltzmann's equation can only describe short time processes. Alder and Wainwright, in a computer calculation of the velocity autocorrelation function for a gas of hard spheres (K system), found that the decay of the autocorrelation function was exponential only for a few mean free times and that after a longer time it decays as a power law. This long tail is derived by a number of authors [20–25] based on the hydrodynamic arguments and the many-body collision considerations. Other explanations, such as the mode-coupling theory, the Brownian-motion theory, and so on, were also presented. However, these techniques all rely on the various approximation scheme. Vivaldi, Casati, and Guarneri [26] analyzed the origin of the long time tails by considering the dynamics of the system in terms of the theoretical arguments and the numerical computations. They discussed a typical strongly chaotic system (K), i.e., the stadium billiard. It is shown that the tails may depend on the presence of arbitrarily long segments of regular motion in the time evolution of the stochastic orbits. Numerical results satisfactorily support this conclusion [26,27].

In our case we study the Boltzmann's entropy rather than the various correlation functions. We find the approaching of the Boltzmann's entropy towards equilibrium value also manifests the long time behavior. For our hard-ball system, the regular-motion mechanism also exists during the free motion and the ball-wall collisions. This should affect the evolution of $H(n_c)$ [or, $\delta(n_c)$]. In Fig. 8, we give the log-log histogram $\delta_p(n_c)$ and $\delta_p(n'_c)$, where n_c denotes the number of collisions of a given ball (i.e., the first ball) with other balls and $\rho_{n'_c}(p)$ as well as $H_p(n'_c)$ are computed at n'_c , i.e.,

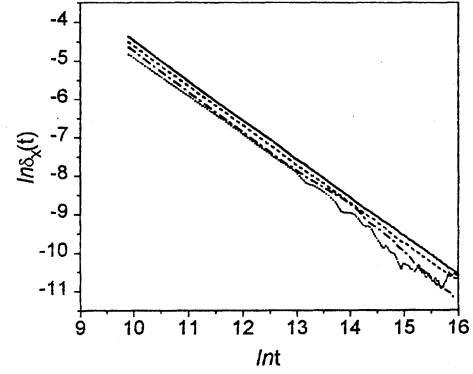


FIG. 10. The log-log (with base $e=2.718\ 281\ 83\dots$) histogram of $\delta_x(t)$ vs t in the two-dimensional motion case for the different radius of balls: $r=5$ (dot-dashed), 10 (dashed), 15 (solid), 20 (dotted). Long straight segments indicates the power-law decay of $\delta_x(t)$.

based on the collisions between the given ball and other balls only. Group A is the same as in Fig. 5, and group B corresponds to the log-log evolution of $\delta_p(n'_c)$. We retain group A in order to give a clear comparison. We find that $\delta_p(n'_c)$ decreases faster than $\delta_p(n_c)$, and a very rapid approach to the equilibriums in the long time regimes occurs in the n'_c cases. These results reveal the effect of the regular motion segments, i.e., it delays the rate of approach to the equilibrium state.

The relaxation in the configuration space can be investigated in a similar way. We may also define the ‘‘Boltzmann's entropy’’ in x space as

$$H_x(t) = \int P_t(x) \ln P_t(x) dx. \quad (9)$$

The relaxation of $H_x(t)$ is plotted in Fig. 9 for a different radius r . Again, $H_x(t)$ decreases monotonically in time, and it approaches its equilibrium value H_{x0} as $t \rightarrow \infty$. In Fig. 10, the log-log histogram of the difference $\delta_x(t) = |H_x(t) - H_{x0}|$ vs time is plotted for a different radius r . It is clearly shown that $\delta_x(t)$ obeys a power-law decay, i.e., $\delta_x(t) \propto t^{-1}$. This is very interesting, because we get the power-law decay in both the momentum space and in the configuration space. The power-law decay in the configuration space is also due to the presence of the arbitrarily long regular segments during the chaotic motion, as may be easily understood from the discussion in the momentum space.

One of the authors (Z.Z.) acknowledges discussions with Professor G. Casati, Professor W. Ebeling, Professor A. Scotti, and Dr. I. Grosse and he thanks them for their useful suggestions. This work is supported by National Natural Science Foundation of China and Nonlinear Science Project.

- [1] Ya. G. Sinai, *Dynamical Systems II, Ergodic Theory with Applications to Dynamical Systems and Statistical Mechanics* (Spring-Verlag, Berlin, 1989).
 [2] R. Jancel, *Foundations of Classical and Quantum Statistical Mechanics* (Pergamon, Oxford, 1969).

- [3] N. S. Krylov, *Works on the Foundations of Statistical Physics* (Princeton University Press, Princeton, NJ, 1979).
 [4] Ya. G. Sinai, *Usp. Mat. Nauk* **25**, 141 (1970) [*Russ. Math. Surv.* **25**, 137 (1970)].
 [5] Ya. G. Sinai, N. I. Chernov, *Usp. Mat. Nauk* **42**, 153 (1987)

- [Russ. Math. Surv. **42**, 150 (1987)].
- [6] V. L. Berdichevsky and M. V. Alberty, *Phys. Rev. A* **44**, 858 (1991).
- [7] V. L. Berdichevsky, *J. Appl. Math. Mech.* **52**, 738 (1988).
- [8] L. E. Reichl, *The Transition to Chaos, In Conservative Classical Systems: Quantum Manifestations* (Springer-Verlag, Berlin, 1992).
- [9] R. Z. Sagdeev, D. A. Usikov, and G. M. Zaslavsky, *Nonlinear Physics, From the Pendulum to Turbulence and Chaos* (Harwood, Academic, Chur, Switzerland, 1988).
- [10] L. Boltzmann, *Lectures on Gas Theory* (Translation from German) (University of California Press, Berkeley, 1964).
- [11] J. W. Gibbs, *Elementary Principles in Statistical Mechanics* (Dover, New York, 1902).
- [12] D. Szasz, *Physica A* **194**, 86 (1993).
- [13] A. Kramli, N. Simanyi, and D. Szasz, *Nonlinearity* **2**, 311 (1989).
- [14] A. Kramli, N. Simanyi, and D. Szasz, *Commun. Math. Phys.* **129**, 535 (1990).
- [15] A. Kramli, N. Simanyi, and D. Szasz, *Ann. Math.* **133**, 37 (1991).
- [16] A. Kramli, N. Simanyi, and D. Szasz, *Commun. Math. Phys.* **144**, 107 (1992).
- [17] G. J. Ackland, *Phys. Rev. E* **47**, 3268 (1993).
- [18] Zhigang Zheng, Gang Hu, and Juyuan Zhang, *Phys. Rev. E* **52**, 3440 (1995).
- [19] L. E. Reichl, *A Modern Course in Statistical Physics* (University of Texas Press, Austin, 1980).
- [20] B. J. Alder and T. E. Wainwright, *Phys. Rev. Lett.* **18**, 988 (1967).
- [21] M. H. Ernst, E. H. Hauge, and J. M. Van Leeuwen, *Phys. Rev. A* **4**, 2055 (1971).
- [22] S. T. Choh and G. E. Uhlenbeck, *The Kinetic Theory of Dense Gases*, dissertation (University of Michigan, 1958).
- [23] J. R. Dorfmann and E. D. G. Cohen, *Phys. Rev. A* **6**, 776 (1972).
- [24] J. W. Dufty, *Phys. Rev. A* **5**, 2247 (1972).
- [25] H. Van Beijeren, *Rev. Mod. Phys.* **54**, 195 (1982).
- [26] F. Vivaldi, G. Casati, and I. Guarneri, *Phys. Rev. Lett.* **51**, 727 (1983).
- [27] R. Brown, E. Ott, and C. Grebogi, *J. Stat. Phys.* **49**, 511 (1987).